Scientific paper

Statistical Optimization of As(V) Adsorption Parameters onto Epichlorohydrin/Fe_3O_4 Crosslinked Chitosan Derivative Nanocomposite using Box-Behnken Design

Vijayanand Nagarajan,[1,*] Raja Ganesan,[1] Srinivasan Govindan[2] and Prabha Govind[3]

[1] *Anna University,Faculty of Chemistry, Paavai Engineering College, Namakkal 637018, TN, INDIA*

[2] *Anna University,Faculty of Chemical Engineering, Paavai Engineering College, Namakkal 637018, TN, INDIA*

[3] *Anna University,Department of Applied Science and Technology, Alagappa College of Technology, Chennai 600005 INDIA*

** Corresponding author: E-mail: vijayanandnagarajanpec@paavai.edu.in*
Phone: +91 8344488356

Received: 06-07-2021

Abstract

In this study, Box-Behnken design (BBD) in response surface methodology (RSM) was employed to optimize As(V) removal from an aqueous solution onto synthesized crosslinked carboxymethylchitosan-epichlorohydrin/Fe_3O_4 nanaocomposite. The factors like solution pH, adsorbent dose, contact time and temperature were optimized by the method which shows high correlation coefficient (R^2 = 0.9406), and a predictive quadratic polynomial model equation. The adequacy of the model and parameters were evaluated by analysis of variance (ANOVA) with their significant factors of Fischer's *F*-test ($p < 0.05$). Seven significant parameters with interaction effects in the experiment with p-value < 0.0001 was observed, having a maximum removal efficiency of As(V) is 95.1%. Optimal conditions of dosage, pH, temperature, initial ion concentration and contact time in the process were found to be 0.7 g, pH 6.5, 308K, 10 mg/L and 60 min respectively. Langmuir isotherm model fitted better than the Freundlich model having a maximum adsorption capacity of 28.99 mg/g, a high regression value of 0.9988, least chi-square value of 0.1781. The process was found to follow monolayer adsorption and pseudo-second-order kinetics. Thermodynamic parameters indicate the process is spontaneous, endothermic and physisorption in nature. Successful regeneration of the adsorbent implies its applicability to the removal of arsenic from real life wastewater.

Keywords: Biosorption; isotherm; kinetics; thermodynamic; optimization; response surface methodology.

1. Introduction

Arsenic is a pervasive element in the environment and has been known as a notorious toxic substance to man and living organisms for centuries.[1] Groundwater Arsenic is primarily associated with oxidative weathering and geochemical reaction of reactive carbon induce mobilization of arsenic in the sediments.[2] Arsenic contaminated groundwater affects over 100 million people in Bangladesh, West Bengal, China, Mexico, Chile, Myanmar, and United states.[3] Long term exposure to arsenic in drinking water causes skin diseases (pigmentation, dermal hyperkeratosis, skin cancer), cardiovascular, neurological, renal, respiratory and black foot diseases, as well as lung, liver, kidney and prostate cancers.[4] To protect public health, the World Health Organization has set a provisional guideline limits of 10 µg/L for arsenic in drinking water which was afterward adopted by the European Union and India.[5] The removal of Arsenic by Co-precipitation, flotation, ion-exchange, ultra-filtration, and reverse osmosis[6] have been received more attention due to its high concentration efficiency.[6] Several adsorbents have been found suitable for arsenic removal counting activated carbon,[7] activated alumina,[8] red mud,[9] etc., In the last decade developments in the knowledge of biosorption exposed high adsorption capacities, low costs and regenerability of natural biosorption materials.[10] However, challenges encountered for biosorbents with high uptake, low cost and as well as in understanding the mechanism of reaction. Chitosan is produced from N-deacetylation of chitin, available from

seafood processing wastes, having hydroxyl and amine group promises good sorption capacity for heavy metal ions through complexation reaction.[11] However, in practical applications it requires a chemical modification to improve the nature of hydrophilic property and adsorption capacity. Carboxymethyl chitosan (CMC) is an amphiprotic chitosan derivative, having hydroxyl (-OH), carboxyl(-COOH) and amine (-NH_2) groups in the molecule can be a substitute for chitosan. But, its poor chemical stability[12] can be overcome by crosslinking reaction with the agents like, glutaraldehyde, glyoxal, and ethylene glycol diglycidyl ether(EDGE), but these cross-linking agents block the amino (NH_2) functional group in CMC backbone.[13] Therefore, epichlorohydrin (EPC) as a mono functional cross linking agent was an effective substitute that will not bind to amino groups in CMC biopolymer and improve the hydrophilic property of CMC and provide enough adsorption sites for increasing adsorption capacity.[14] However, the fact of high desirability exist between inorganic arsenic species and iron[15] tends to advance the utility of Fe (III)-bearing materials like hematite,[16] ferrihydrite,[17] and iron-doped activated carbons for arsenic adsorption.[18] Thus, the objective of the present study is to prepare and evaluate a hybrid composite biopolymer of crosslinked epichlorohydrin/Fe_3O_4 nanocomposite (CMC-EPC/INC) for removal of As(V). RSM is a multivariate technique employed to reduce the number of experimental runs required to provide sufficient information for statistically acceptable results.[19] Hence the parameters such as adsorbent dosage, initial metal ion concentration, solution pH, working temperature were optimized through Box-Behnken design model (BBM), which provide an insight of parameters level for maximum performances.[20] The Langmuir and Freundlich isotherm models were applied to evaluate the adsorption equilibrium. Kinetic studies, thermodynamic property and desorption experiments were carried and discussed.

2. Experimental

2. 1. Material

Carboxymethylchitosan (CMC, MW = 2.65×10^5), Epichlorohydrin (EPC), Ferric chloride hexahydrate ($FeCl_3$ $6H_2O$), Ferrous chloride tetrahydrate ($FeCl_2 \cdot 4H_2O$), Sodium hydrogen arsenate (Na_2HAsO_4 $7H_2O$),1-ethyl-3-carbodiimide hydrochloride (EDC), N-hydroxyl succinimide (NHS), Sodium hydroxide and acetic acid were of analytical grade, acquired from Sigma Aldrich. Stock As(V) solution (1000mg/L) were prepared from sodium hydrogen arsenate. All the reagents and glassware were prepared with de-ionized water.

2. 2. Preparation of Fe_3O_4 Nanoparticles

Fe_3O_4 nanoparticles synthesized,[21] by taking 0.02 moles of $FeCl_3.6H_2O$ and 0.01moles of $FeCl_2$ $4H_2O$ dissolved in 100 mL of deionized water at 30 °C, under vigorous stirring precipitation occurs by the addition of 1M NaOH after 60min. Then it was heated to 60 °C for 3h under the pH ± 12. After cooled the solution to room temperature, the precipitate was collected by a magnet and washed with deionized water until the pH reached neutral. Finally, it was washed with acetone and dried in an oven at 60 °C for 24h.

2. 3. Synthesis of CMC-EPC/Fe_3O_4 Nanocomposite

1g of CMC was dissolved in acetic acid (50 mL, 5% v/v), and the mixture was sonicated at room temperature for 3 h.Then 0.6 g of magnetic nanosized ferroferric oxide was added and left it for 24 h at room temperature with vigorous stirring to ensure complete mixing. Beads of CMC-Fe_3O_4 (MCMC) formed when the resultant solution was injected into a 100 mL sodium hydroxide (0.5 M) by syringe needle (10 mL) as drops, and washed with distilled water plenty for the removal of excess sodium hydroxide solution. The crosslinking steps were carried out by dissolving 1 g of MCMC beads in 60 mL of ultrapure water followed by adding 0.6 g of EDC and 0.8 g of NHS at pH 5–6 inorder to activate the carboxyl groups of MCMC. After 1 h, 1% epichlorohydrin (100 mL) was added to the beads with gentle stirring in water bath at 40 °C for 24 h. Then the crosslinked (CMC-EPC/INC) beads were washed many times by distilled water, air dried and grinded using mortar and dried constantly in the oven. Finally, the prepared adsorbent was sieved to a particle size < 250μm for study.

2. 4. Batch Adsorption Experiments

Batch experiments were carried out with 50mL of As(V) solution having an initial concentration of 10 mg/L. The investigation of parameters are temperature (20–50 °C), pH (2–10), reaction time (5 min–5 h), and adsorbent dosage (0.1–2g/50 mL) in order to find the maximum uptake of arsenic ions. Samples were collected at fixed intervals and the adsorbent was removed by centrifugation at 6000 rpm for 6 min. The supernatant was analyzed for As(V) removal by AAS. Blanks were used for control in all the experiments. The amount of arsenic adsorbed (mg/g) was determined by the following equation.

$$qe = (C_o - C_e) \times \upsilon/_m \quad (1)$$

Where C_0 and C_e are the initial and equilibrium concentrations of the metal ion (mg/L), m is the dry mass of iron-doped chitosan (g) and υ is the volume of the solution (L). The % removal of As(V) from aqueous solution was calculated by the following equation;

$$\text{Removal (\%)} = [(C_0 - C_e)/C_0] \times 100 \quad (2)$$

2. 5. Experimental Design

Response surface methodology (RSM) with Box–Behnken design (BBD) was employed to determine the effect of four independent variables. The effect of parameters including temperature (x_1), pH (x_2), reaction time (x_3), and adsorbent dosage (x_4) were analysed. For data analysis, design expert software (Stat Ease, Inc., Version 11, USA) was used. By batch experiments.The following equation explain the coded values of the process variables.

$$X_i = \frac{(x_i - x_{oi})}{\Delta xi},\ i = 1,2,3 \ldots \ldots \ldots k \quad (3)$$

Where X_i and x_i are the coded and uncoded values of the i_{th} variables, x_{oi} denotes the uncoded values of the i_{th} ariable at the center point, and Δx_i is the step change value. The process parameters were optimized by 29 experimental runs and the levels of parameters used in the adsorption process were summarized in Table 1. The % removal of As(v) was determined by the following second order polynomial equation.

$$Y = \beta_0 + \sum_{i=1}^{4} \beta_i x_i + \sum_{i=1}^{4} \beta_{ii} x_i^2 + + \sum_{i,j=1(i=j)}^{4} \beta_{ij} x_i x_j + \varepsilon \quad (4)$$

Where Y is the response variable, βo, βi, βij, and βii, are the regression coefficients for intercept, linear effect, double interaction, and quadratic effects, respectively, x_i, x_j are the independent variables, and ε is a random error. Statistical analysis system software was used for the study of Analysis of variance (ANOVA), response surface studies and 3D surface plot generation.

Table 1. Factors and level of various parameters of BBM design for As(V) adsorption

Parameters		Level of factors		
Variables	Code	−1	0	1
Temperature (°C)	x_1	30	35	40
pH	x_2	5	6.5	8
Contact time(min)	x_3	45	60	75
Adsorbent dosage(mg L^{-1})	x_4	600	700	800

2. 6. Analytical Measurements

Micromeritics ASAP 202 analyzer, pH-potentiometric titration method, reported by Vieira and Beppu,[22] was carried out to determine the porosity and amino group content in the biosorbent respectively. Shimadzu AA 7000 model atomic absorption spectrometer (AAS) was used to find the concentration of adsorbed arsenic at 193.7nm with an air-acetylene flame type.[23]

3. Results and Discussion

3. 1. Porosity and Potentiometric Analysis

The adsorbent has BET analysis surface area of 2.85 (m^2/g). Surface morphology of the composite indicates, Fig. S1 (a), that the adsorbent is porosity with more white patches, Fig.S1(b), indicates that the adsorbent complexes with arsenic ions after the adsorption. The cross-linking of EPI,[24] reacts with the primary alcoholic group (-CH_2OH) at position C-5 of CMC's pyranose ring thus indicated that the amino (-NH_2) group plays a major role in the adsorption of arsenic anion by electrostatic attraction.[25]

3. 2. FTIR Analysis

The FTIR spectra of the pure CMC, CMC-EPI/INC before and after As(V) adsorption were displayed in Fig. 1.

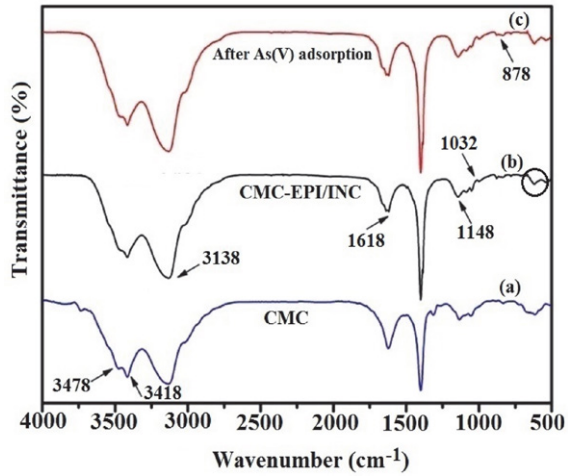

Fig. 1. FT-IR spectra of a) CMC b) CMC-EPI/INC before and C) after As(V) adsorption

The IR spectrum of CMC in Fig.1 (a), show peaks at 3478 cm^{-1}, 3418 cm^{-1}, 3138 cm^{-1} and 1618 cm^{-1} were attributed to the symmetrical, asymmetric stretching vibration of and –NH_2 group and stretching vibration of O-H, with the effect of hydrogen bonds, and C = O in amide respectively. The peaks at ~1148 cm^{-1} and ~1032 cm^{-1} in Fig.1(b), corresponds to stretching of C-O-C and C-O bonds respectively, resulted in the formation of covalent bonds due to reaction between EPI with the carbon atoms in CMC, which causes the opening of the epoxide ring of EPI and the releasing of a chlorine atom.[26] The bands around 600–700 cm^{-1} is assigned to the bending vibration of Fe-O-Fe bond. The appearance of new band ~878 cm^{-1} shown in Fig.1 (c), corresponds to the existence of arsenic anion.

3. 3. Equilibrium Isotherm

The equilibrium parameters of adsorbent dosage, pH, temperature, initial ion concentration and contact

time were found to be 0.7 g, pH 6.5, 308 K, 10 mg/L and 60 min, respectively and found that the reaction takes place by diffusion and complexation process.[27]

3. 4 Quadratic Model for As(v) Adsorption

The BBM technique were employed for the optimization of As(v) adsorption capacity.Table 2, displays the 29 runs of experimental design, along with corresponding adsorption results. The removal efficiency as functions parameters was correlated with the developed second-order polynomial equation. The empirical model in terms of process variables, is expressed by the following equation.

The effect of independent variables on the adsorption efficiency of As(V) was described by the equation shown above.The amount of maximum As(V) adsorption was found to be 95.1%. Experimental curve fitting was evaluated to govern the apparent model by calculating

$$\% \text{ removal of As(v)} = -203.02898 + 8.97600 + 22.29704 + 0.188444 + 0.153967 - 0.023333 - 0\ .001333 + 0.000150 + 0.038889 - 0.005167 + 0.000233 - 0.122133 - 1.55148 - 0.004293 - 0.000095 \quad (5)$$

Table 2. Experimental design of variables with adsorption results

Std	Run	Coded levels x_1	x_2	x_3	x_4	Removal of As(v)%
21	1	35	3	60	600	88.1
1	2	30	3	60	700	86.3
12	3	40	4.5	60	800	93.1
26	4	35	4.5	60	700	95.1
17	5	30	4.5	45	700	87.8
14	6	35	6	45	700	88.4
27	7	35	4.5	60	700	95.1
29	8	35	4.5	60	700	95.1
6	9	35	4.5	75	600	92.6
25	10	35	4.5	60	700	93.8
4	11	40	6	60	700	90.2
24	12	35	6	60	800	90.4
15	13	35	3	75	700	91.1
8	14	35	4.5	75	800	93.4
9	15	30	4.5	60	600	89.2
20	16	40	4.5	75	700	92.9
22	17	35	6	60	600	89.5
23	18	35	3	60	800	92.1
2	19	40	3	60	700	89.6
19	20	30	4.5	75	700	89.8
10	21	40	4.5	60	600	91.8
5	22	35	4.5	45	600	93.4
11	23	30	4.5	60	800	90.2
18	24	40	4.5	45	700	91.3
13	25	35	3	45	700	90.7
28	26	35	4.5	60	700	95.1
16	27	35	6	75	700	92.3
3	28	30	6	60	700	87.6
7	29	35	6.5	45	800	92.8

larger *F*-and lower probability values (*p*-values) with significant terms were chosen. From the data given in Table 3, a quadratic model was suggested for higher *F*- value (40.7) and lower *p*-value (<0.0001) with significant terms for this experimental design. The cubic model was found to be insignificant.The significance of the quadratic model was justified by ANOVA by correlating with the response variables such as the main effects, the interaction effects, and the error terms. The *F* and *p* values represented the enormousness of these variables. BBD was adopted to design 29 experiments (Table 4) for investigate the individual and interactive effects of the four independent variables on removal of As(V). The experimental data of As(V) removal, were statistically analyzed by analysis of variance (ANOVA) and the results are presented in Table 4.

From the Table 4, the *F*- value of 15.84 indicated that the model was statistically significant and there is only a 0.01% chance that an *F*-value this large could occur due to noise. The model suggested was highly significant due to its *p*-value of <0.0001. The Table 4, shows the seven significant terms with low *p*-values were x_1, x_3, x_4, x_1^2, x_1^2, x_2^2, x_3^2, and x_4^2. Other significant terms were not discussed because of their high *p*-values. The above model accuracy could be assessed by the fortitude of regression coefficient R^2 value 0.9406, indicated that only 6% of the total variables were not explained by the model.

The adjusted coefficient value (R^2_{adj} = 0.8813) was not in realistic arrangement with observed R^2. The model has undesirable lack of fit by the indication of lack of fit *p*-value (>0.05) suggested that it is not significantly relative to the pure error and, thus, above quadratic equation and the model were accurate for the experiment.[28] The

Table 3. Experimental curve fitting of optimization

Model	Sum of Source	DF	Mean Squares	*F*-Square	*p*-value	Remarks value
Linear vs Mean	36.53	4	9.13	1.64	0.1976	–
2FI vs Linear	6.14	6	1.02	0.15	0.9879	–
Quadratic vs 2FI	117.65	4	29.41	40.70	< 0.0001	Suggested
Cubic vs Quadratic	7.06	8	0.89	1.74	0.2589	Aliased

Table 4. Analysis of variance for the model by BBM optimization for As(v) adsorption

Source	DF	Mean Square	*F*-value	*p*-value	Remarks
Model	14	11.45	15.84	< 0.0001	significant
x_1 (°C)	1	27.00	37.36	< 0.0001	significant
x_2 (pH)	1	0.0208	0.0288	0.8676	–
x_3 (min)	1	4.94	6.84	0.0204	significant
x_4 (mg)	1	4.56	6.31	0.0248	significant
x_1x_2	1	0.1225	0.1695	0.6868	–
x_1x_3	1	0.0400	0.0553	0.8174	–
x_1x_{24}	1	0.0225	0.0311	0.8625	–
x_2x_3	1	3.06	4.24	0.0587	–
x_2x_4	1	2.40	3.32	0.0897	–
x_3x_4	1	0.4900	0.6780	0.4241	–
x_1^2	1	60.47	83.68	< 0.0001	significant
x_2^2	1	79.04	109.37	< 0.0001	significant
x_3^2	1	6.05	8.37	0.0118	significant
x_4^2	1	5.90	8.16	0.0127	significant
Residual	14	0.7227	–	–	–
Lack of Fit	10	0.8766	2.59	0.1858	not
significant					
Pure Error	4	0.3380	–	–	–

value of signal to noise ratio is 13.511, ratio >4 is desirable, indicated an adequate signal to navigate the design space.[29] The Fig. 2a graph, plotted between actual and predicted values shows no apparent violation from the assumptions underlying of the analyses,[30] indicated that the distribution of actual values were relatively close to the straight line, specify the accuracy of the assumptions, as well as the independence of the residuals. The plot between studentized residuals and run number, in Fig. 2b, showed that the random distribution of residuals around ± 3.9 (limit is < ±4.00) was a good sign of well fitted experimental data with the model.[31]

3. 5. Effect of Process Variables on Removal of As(v)

The optimization process parameters and the interaction between the variables were studied by a plot of three-dimensional curves for the efficient adsorption of As(V). Fig. 3a, represents the effect of temperature and pH

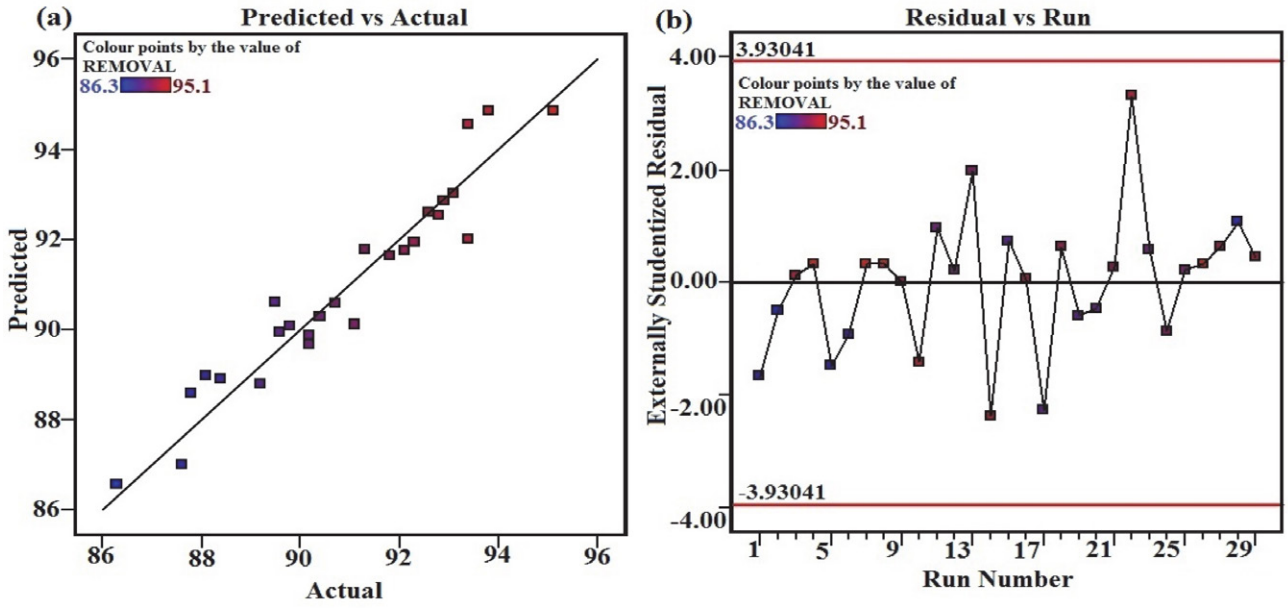

Fig. 2. RSM model graphs of a) Predicted vs Actual values b) Studentized residuals vs experimental run number on optimized parameters of As(V) removal

indicated that the adsorption reaches maximum at 35 °C on pH 6.5 beyond that desorption process start and continues due to complexation. Fig. 3b represents the correlation of temperature and reaction time having optimal adsorption efficiency of 95.1% was reached within 60 min at temperature of 35 °C, beyond that contact time (>60 min) and temperature (>35 °C), the adsorption rate decreased. The plot of temperature versus adsorbent dosage in Fig. 3c, shows that the degree of adsorption increases with increasing adsorbent dosage, upto 700 mg on 35 °C, due to high surface availability, beyond 800 mg dosage and 35 °C it has equilibrium and decreasing trend continues infers, that the process is controlled by temperature.[32] Fig. 3d, shows the effect of time and pH and the adsorption capacity was almost constant in the pH range 5–6, and then increases and reaches maximum at pH 6.5, which matches with the pKa value of chitosan.[33] From the above it was evident that the adsorption rate mainly depends on temperature and pH, while the contact time had fringe effect only. The above fact is supported by the contour plot,[34] in Fig. S2, between pH and temperature had a difference minimum 0.5% between experimental and predicted removal efficiency shows that the adsorption is endothermic took place by the increasing diffusion rate and the growing rate of complexation between adsorbent and adsorbate.[35]

3. 6. Langmuir Isotherms

The isotherm models employed describes the sorption data, sorption mechanism, the surface properties and the affinity between sorbent and sorbate.[36] The Langmuir isotherm model represents the monolayer sorption on an

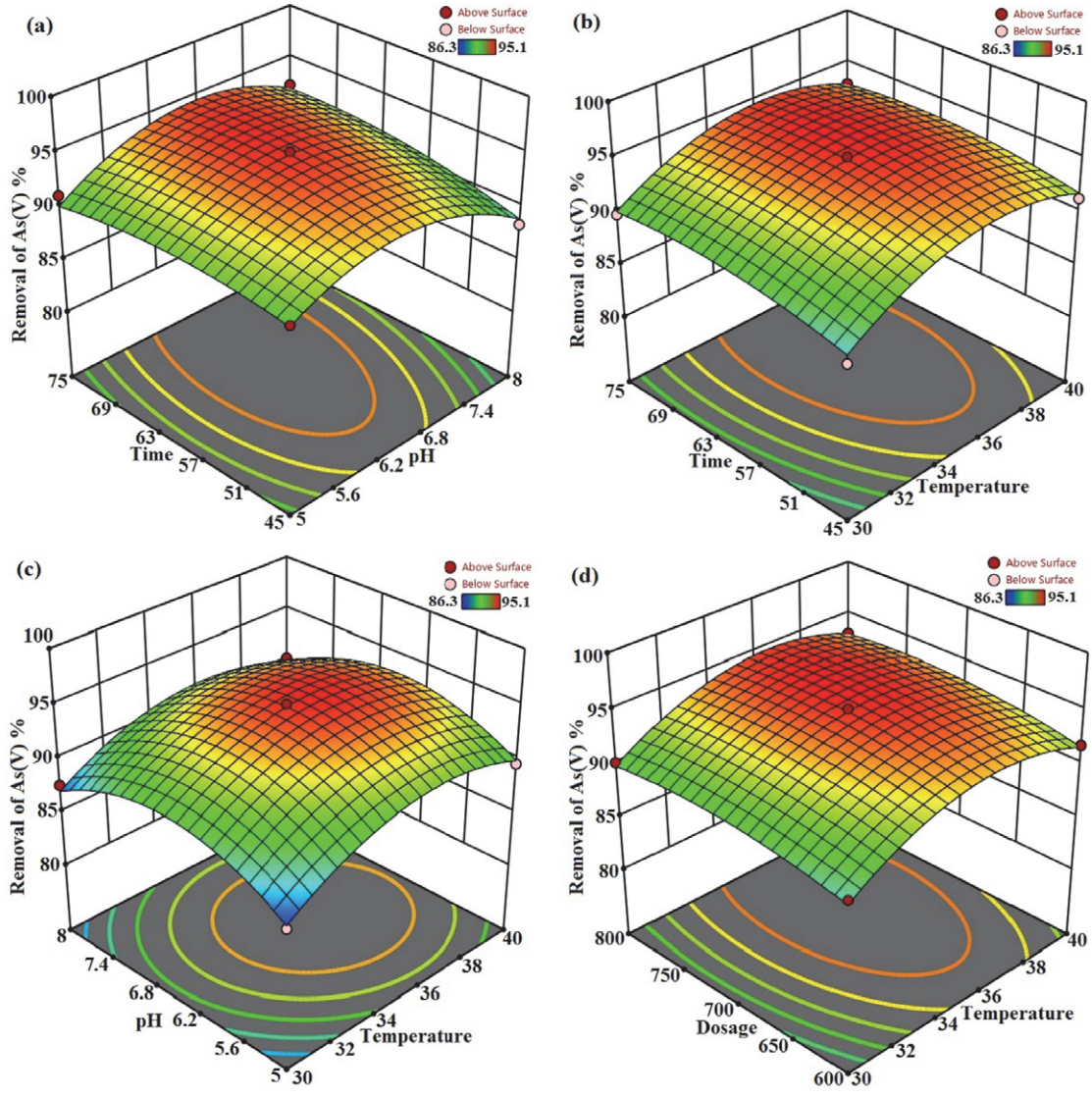

Fig. 3. 3D surface plot of interaction effects between variables of a) time vs pH b) time vs temperature c) pH vs temperature and d) adsorbent dosage vs temperature on As(V) removal

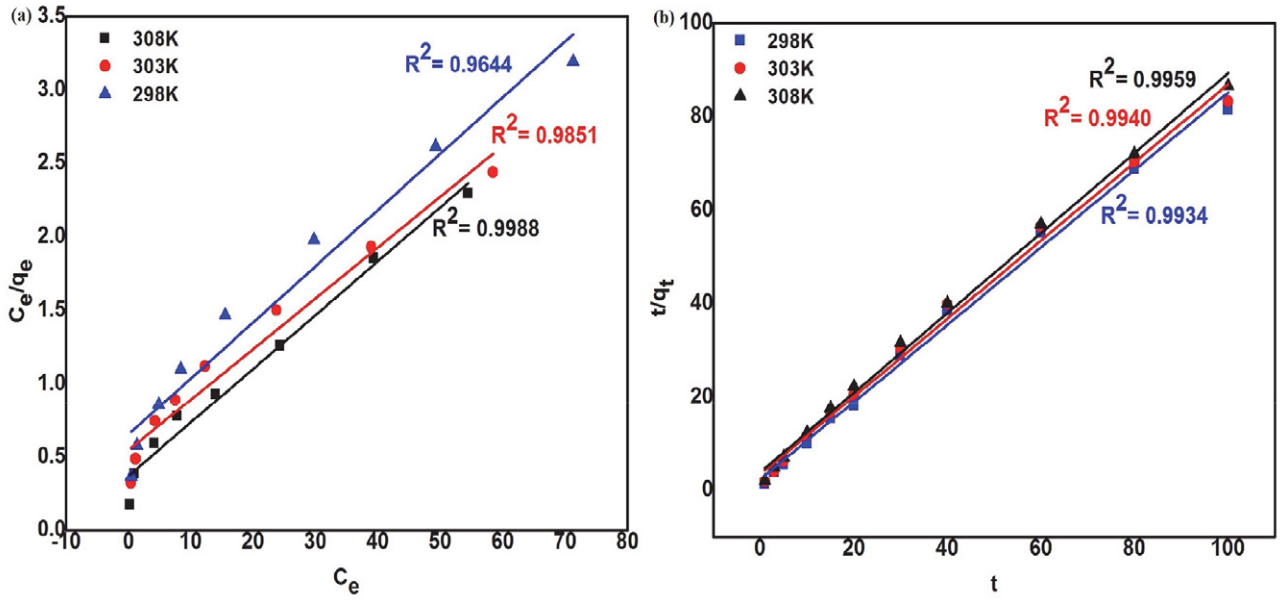

Fig. 4. 3D surface plot of interaction effects between variables of a) time vs pH b) time vs temperature c) pH vs temperature and d) adsorbent dosage vs temperature on As(V) removal

energetically uniform surface having maximum adsorption capacity, q_m = 26.11–28.99 mg g^{-1}, and higher regression coefficient, R^2 = 0.9988 obtained from the relevant plots, Fig. 4a, and Table 5, suggesting that the surface of the sorbent was homogenous. The dimensionless factor (R_L = 1/1 + bC_o) was calculated as <1, indicates favourable and monolayer adsorption process.The certainty of the isotherm were committed by the least RMSE and χ^2 values for Langmuir model than Freundlich model.

3. 7. Freundlich Isotherm

The isotherm describes the sorption on an energetically heterogeneous surface and the exponential distribution of active sites and their energies.[37] The value of n (adsorption intensity) obtained by the Table 5, from the plot (Fig.S3) in the range 1–10 signifies the good performance of Fe_3O_4 doped CMC-EPI adsorbent towards As(V) adsorption.

3. 8. Residual Mean Square Error (RMSE) and Chi-square (χ^2) statistical test

To represent the errors in the isotherm curves the RMSE and *Chi-square (χ^2) statistical* analysis is employed.

$$\text{RMSE} = \frac{1}{n-2}\sum_{i=1}^{n}(qe_{exp} - qe_{cal})^2 \quad (6)$$

qe_{exp}, qe_{cal} and n are the experimental, calculated values and number of observations respectively.[38] The χ^2 test confirms the suitability of a particular isotherm model given by the equaton,[39]

$$\chi^2 = \sum \frac{(qe,\text{exp} - qe,cal)^2}{qe,cal} \quad (7)$$

The RMSE and χ^2 value would be less if the adsorption data correlated concurs with experimental values. By

Table 5. Isotherm parameters for As(v) adsorption on pH = 6.5, adsorbent dosage = 700mg/L,contact time = 60 min at different temperatures onto the CMC-EPI/INC composite

Parameters	Langmuir Temperature (K)			Parameters	Freundlich Temperature (K)		
	298	303	308		298	303	308
$q_{m(mg\,.\,g^{-1})}$	26.11	27.38	28.99	$k_{f(mg\,.\,g^{-1})}$	1.4027	1.4276	1.5327
$k_{1(L\,.\,mg^{-1})}$	0.0594	0.0668	0.0941	η	1.9592	1.6489	1.8221
R^2	0.9644	0.9851	0.9988	R^2	0.9623	0.9821	0.9898
R_L	0.6274	0.5995	0.5152				
RMSE	0.3852	0.3526	0.2978	RMSE	2.9651	3.1475	3.2541
χ^2	0.2943	0.2896	0.1781	χ^2	5.9621	5.6254	4.9632

which, from Table V, the adsorption suitability more correlate with the Langmuir model than other models.

3. 9. Kinetic Study

The kinetics,[40] effective adsorption capacity, initial adsorption rate and the rate constant of As(v) adsorption without any parameter in advance were evaluated using the pseudo First order and Second order equation.[41] The linear form of pseudo-first-order Lagergren equation and pseudo-second-order equation is given as equation 8 and 9.

$$\log (q_e - q_t) = \log q_e - \frac{k_1 t}{2.303} \quad (8)$$

$$\frac{t}{q_t} = \frac{1}{k_2 qe^2} + \frac{t}{qe} \quad (9)$$

The initial adsorption rate, h (mg/(g min)), as $t \rightarrow$ = 0, can be defined as:

$$h = k_{2qe^2} \quad (10)$$

Where, k_1 and k_2 are the rate constant of Pseudo first order and second order equation respectively. The kinetic parameters were obtained through the Pseudo first order plot (Fig.S4), and second order plot (Fig. 4b) shows higher regression coefficient value of 0.996, (Table 6) for the second order model, exposed its applicability in fitting the experimental kinetic data. From the Table 6, it shows that the h value of As(V) adsorption at 35 °C was higher than at 25 °C.

3. 10. Intraparticle diffusion

The Weber-Morris model for intraparticle diffusion, explored the nature of the 'rate-controlling step, which is given by the equation as,[42]

$$q_{id} = k_{id} t^{0.5} + c \quad (11)$$

Where k_{id} is the intraparticle diffusion rate constant ($(mg/g\ min^{0.5})$). From the plots q_e versus $t^{0.5}$, Fig. S5, the relationship is not linear and follows rate-limiting step. The first sharper portion being rapid external surface adsorption, the second portion being gradual adsorption and the final phase being final equilibrium stage due to the low concentration of As(V) in the solution phase as well as less number of available adsorption sites.

3. 11. Adsorption Thermodynamics

The thermodynamic parameters were utilized to elucidate the feasibility of adsorption.[43] The Van't Hoff plot, Fig. 5 (In K_c against 1/T) relates the parameters as

$$\ln K_c = \frac{-\Delta H}{RT} + \frac{\Delta S}{R} \quad (12)$$

$$\Delta G = - RT \ln K_c \quad (13)$$

Where *Kc* is the equilibrium constant, T the absolute temperature (K), and R is the universal gas constant (8.314 J mol^{-1}). The calculated values of the energy parameters ΔG (change in free energy), ΔH (change in enthalpy), and ΔS (change in entropy) are given in the Table 7. The negative ΔG values observed at various temperatures suggested the feasibility and spontaneous adsorption process.

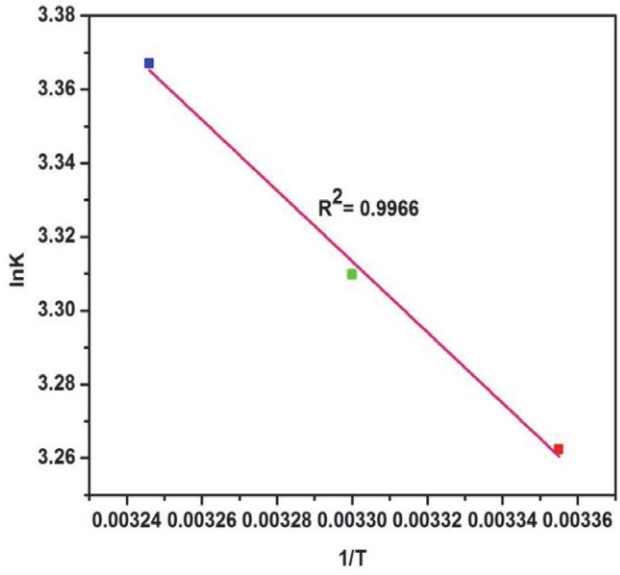

Fig. 5. Van't Hoff plot of As(V) adsorption at different temperatures

Table 6. Kinetic parameters for As(V) adsorption on pH = 6.5, adsorbent dosage = 700 mg/L, contact time = 60 min at different temperatures onto the CMC-EPI/INC composite

Temp (K)	Pseudo first order				Pseudo Second order				Intra particle diffusion
	$q_{e,exp}$ mg/g	$q_{e,cal}$ mg/g	k_1 (min^{-1})	R^2	h (mg . min^{-1})	$q_{e,cal}$ mg/g	k_1 (min^{-1})	R^2	K_{id} ($mg/g \cdot min^{1/2}$)
298	1.1954	1.169	0.019	0.980	0.1957	1.019	0.2326	0.993	0.045
303	1.2015	1.198	0.021	0.987	0.2142	1.128	0.2432	0.994	0.043
308	1.2235	1.035	0.025	0.992	0.2583	1.175	0.1885	0.996	0.040

Table 7. Thermodynamic results of As(V) adsorption at different temperatures

	Van't Hoff plot		
Temp (kJ/mol)	**ΔG (kJ/mol)**	**ΔH (J/mol/k)**	**ΔS**
289K	–8.0787	7.9835	0.0539
303K	–8.3482		
308K	–8.6177		

The positive nature and the value of ΔH = 7.9835!!!!! (< 80 kJ · mol^{-1}) suggesting that the reaction follows endothermic physisorption. The positive value of ΔS reflects the affinity and some structural changes in adsorbent and adsorbate during adsorption process.[44]

3. 12. Desorption Experiments

Desorption studies carried out with 0.1M NaOH, in a batch reactor. The desorption result

(Table S1), revealed that after four cycles around 81–87% of loaded As(V) were found to be

desorbed during desorption cycles. The desorption ratio was calculated by:

$$R(\%) = \frac{C_2}{C_0 - C_1} \times 100\% \quad (14)$$

Where C_0, C_1, and C_2 are the initial, equilibrium concentration of adsorbed and desorbed solution in mg/L respectively.

4. Conclusions

The removal of As(V) were successfully carried out in this study by the prepared novel hybrid crosslinked magnetite enhanced carboxymethylchitosan biosorbent. The optimization results of main variables by Box-Behnken Design of RSM model (R^2 = 0.9406) shows the process were good in agreement with arsenic adsorption. This factorial experimental design approach developed an empirical equation for the prediction and understanding of As(V) adsorption efficiency.The model outcome with seven siginificant figures, maximum removal efficiency of 95.1%, with 0.5% difference between actual andpredicted values.The interaction effect results infers the most influencing parameters are pH and temperture while contact time and adsorbent doage are the least influencing parameters.The maximum sorption capacity for As(V) was calculated to be 28.99 mg g^{-1} from the Langmuir isotherm, correlate with low RMSE and chi square value, and follows pseudo-second-order kinetics. Thermodynamic studies revealed the process is spontaneous, endothermic and physisorption in nature. Interfering ions had minimal effects on adsorption. The adsorbent was successfully recycled for four cycles and efficiently treated with As (V) contaminated wastewater. Thus, it could be concluded that the CMC-EPI/INC biosorbent would be a prospective candidate for arsenic filtering units, due to its biocongenial nature.

Acknowledgment

The authors also would like to thank Department of Chemistry, IIT Madras and Center for Environment, CLRI Chennai for providing the analytical instrumentation facility. One of the authors Dr.G.Prabha would like to thank University Grant Commission (UGC), Government of India, for providing the fund under the scheme of UGC – Dr. D.S. Kothari Postdoctoral Fellowship (Award No:F.4-2/2006(BSR)/CH/18-19/0110).

Conflict of interest

As the author(s), we declare that there is no conflict of interest regarding the publication of this article.

5. References

1. A. K. Sharma, J. C. Tjell J. C, J. J. Sloth, P. E. Holm, *Appl. Geochem,* **(2014)**,*41*:11–33. **DOI:**10.1016/j.apgeochem.2013.11.012
2. S. Fendorf, H. A. Michael, A.Geen, *Science Mag,* **(2010)**, *328 (5928),* 1123–1127. **DOI:**10.1126/science.1172974
3. P. L. Smedley, D. G. Kinniburgh, *Appl. Geochem,* **(2002)**, *17,* 517–568. **DOI:**10.1016/S0883-2927(02)00018-5
4. W. E. Morton, D. A.Dunette, Arsenic in the Environment, Part II, *Wiley and sons,*New York **(1994)**, 17–34. **DOI:**10.1002/jat.2550150320
5. Drinking water Quality Information, *World Health Organization,*Vol 2,WHO,Geneva **(1984)**, 940–949. **DOI:**10.1002/food.19860300121
6. V. M Boddu, K. Abburi, J. L.Talbott, E. D. Smith, R.Haasch, *Water. Res,* **(2008)**, *42,* 633–642. **DOI:**10.1016/j.watres.2007.08.014
7. A. Dabrowski, Z. Hubicki, P. Podkościelny, E. Robens, *Chemosphere*, **(2004)**, *56(2)*, 91–106. **DOI:**10.1016/j.chemosphere.2004.03.006
8. T. F. Lin, J. K. Wu, *Water Res,* **(2001),** *35(8),* 2049–2057. **DOI:**10.1016/S0043-1354(00)00467-X
9. H. Genc-Fuhrman, J. C. Tjell, D. McConhie, *J. Colloid Interface Sci,* **(2004)**,*27(2)* 313–320. **DOI:**10.1016/j.jcis.2003.10.011
10. F. Fu, Q.Wang, *J. Envn Mgmt*, (2011), 92(3), 407–418. **DOI:**10.1016/j.jenvman.2010.11.011
11. R. S. Juang, F. C. Wu, R. L. Tseng, *Water Res,* **(1999)**, *33(10),* 2403–2409. **DOI:**10.1016/S0043-1354(98)00469-2
12. P. Pillewan, S. Mukherjee, T. Roychowdhury, S. Das, A. Ban-

siwal, S. Rayalu, *J.Hazard. Mater*, **(2011)**, *186 (1)*, 367–375. **DOI:**10.1016/j.jhazmat.2010.11.008
13. M. Bilal, Z. Jing, Y. Zhao, H. M. Iqbal, *Biocatal. Agric. Biotechnol,* **(2019)**, *19,* 101174 –101184. **DOI:**10.1016/j.bcab.2019.101174
14. Y. Gutha, Y. Zhang, W. Zhang, X. Jiao, *Int. J. Biol. Macromol,* **(2017)**, *97,* 85–98. **DOI:**10.1016/j.ijbiomac.2017.01.004
15. F. Marrakchi, W. A. Khanday, M. Asif, B. H. Hameed, *Int. J. Biol. Macrol,* **(2016)**, *93(pt A),* 1231–1239. **DOI:**10.1016/j.ijbiomac.2016.09.069
16. K. P. Raven, A. Jain, R. H. Leoppert, *Environ. Sci. Technol,* **(1998)**, *32(3),* 344–349. **DOI:**10.1021/es970421p
17. V. Fierro, G.Muniz, M. L. Ballinas, *J. Hazard. Mater,* **(2009)**, *168(1),*430–437. **DOI:**10.1016/j.jhazmat.2009.02.055
18. H. Genc-Fuhrman, J. C. Tjell, D. McConchie, *Environ.Sci. Technol,* **(2004)**, *38(8),* 2428-2439. **DOI:**10.1021/es035207h
19. A. H. Jawad, N. N. Abd Malek, A. S. Abdulhameed, R. Razuan, *J. of Polymers and the Environ,***(2020)**, *28*, 1068–1082. **DOI:**10.1007/s10924-020-01669-z
20. A. Reghioua, D. Barkat, Ali H. Jawad, A. S. Abdulhameed, A. A. Al-Kahtani, Z. A. Alothman, *J. of Environ. Chem. Eng,* **(2021)** *9(3)*,105166. **DOI:**10.1016/j.jece.2021.105166
21. T. S. Anirudhan, L. Divya, J. Parvathy, *Journal of Chemical Technology & Biotechnology*, **(2013)**, *88(5)*, 878–886. **DOI:**10.1002/jctb.3916
22. R. S. Vieira, M. M. Beppu, *Coll .Surf. A,* **(2006)**, *279(1–3),*196–207. **DOI:**10.1016/j.colsurfa.2006.01.026
23. E. Guibal, T.Vincent, R. Navarro, *J. Mater. Sci,* **(2014)**, *49,* 5505–5518. **DOI:**10.1007/s10853-014-8301-5
24. Y. Haldorai, T. Rengaraj, Y. S. Huh, Y. K. Han, *Mater. Sci. and Eng B,***(2015)**,*136921,*01–10. **DOI:**10.1016/j.mseb.2015.01.006
25. A. T Mohammad, A. S. Abdulhameed, A. H. Jawad, *Int. J. Macromol,* **(2019)**, *129,*98–109. **DOI:**10.1016/j.ijbiomac.2019.02.025
26. K. Manzoor, M. Ahmad, S. Ahad, S. Ikram, *RSC Adv,* **(2019)**, *9,* 7890–7902. **DOI:**10.1039/C9RA00356H
27. M. Monier, D. A. Abdel-Latif, *Int. J. Biol. Macromol,* **(2017)**, *105(1),* 777–787. **DOI:**10.1016/j.ijbiomac.2017.07.098
28. J. L. Wang, C. Chen, *Biotechnol Adv,* **(2009)**, *27,* 195–226. **DOI:**10.1016/j.biotechadv.2008.11.002
29. E. Guibal, *Purif. Technol,* **(2004)**, *38(1),*43–74. **DOI:**10.1016/j.seppur.2003.10.004
30. Ali H. Jawad, I. A. Mohammed, A. S. Abdulhameed, *J of Poly and the Environ,* **(2020),** *28*,2720–2733. **DOI:**10.1007/s10924-020-01804-w
31. N. Ayawei, A. T. Ekubo, D. Wankasi, E. D. Dikio, *Oriental. J. of Chem,* (2015), *5(03),*56–70. **DOI:**10.4236/ojpc.2015.53007
32. S. Sharma, M. Bharathi, and N. Rajesh, *Chemical Eng. J,* **(2015)**, *59,* 457–466. **DOI:**10.1016/j.cej.2014.08.002
33. C. Chia-Pin, L. Ming-Chao, L. Chung-Min, *J. of Hazard. Mater,* **(2009)**, *171(1–3),*859–864. **DOI:**10.1016/j.jhazmat.2009.06.086
34. Ali H. Jawad, Ahmed Saud Abdulhameed, Nurul Najwa Abd Malek, Zeid A. ALOthman, M. *Inter. J. of Bio. Macromol,***(2020)**,*164(020)* 4218–4230. **DOI:**10.1016/j.ijbiomac.2020.08.201
35. H. Guo H. Y. Li, K. Zhao, *J. of Hazard Mater,* **(2010)**, *176(1–3),*174–180. **DOI:**10.1016/j.jhazmat.2009.11.009
36. C. Yuwei, W. Jianlong, *Chemical Eng. J,* **(2011)**, *168(1),* 286–292. **DOI:**10.1016/j.cej.2011.01.006
37. G. E. J. Poinern, D. Parsonage, B. Touma B, M. K. Issa Ghosh, E. Paling, P. Singh, *Inter. J. of Eng Sci. and Technol,* **(2010)**, *2(8),* 13–24. **DOI:**10.4314/ijest.v2i8.63776
38. A. S. Krishna Kumar, C. Uday Kumar, R. Vidhya, N. Rajesh, *Inter. J. of Biological macromol,* **(2014)**, *66,*135–143. **DOI:**10.1016/j.ijbiomac.2014.02.007
39. G. Anjali, M. Yunus, S. Nalini, *Chemosphere. (2012),86(2),* 150–155. **DOI:**10.1016/j.chemosphere.2011.10.003
40. B. Choudhary, D. Paul, *J. Environ. Chem. Eng.* **(2018)**, *6(2),* 2335–2343. **DOI:**10.1016/j.jece.2018.03.028
41. K. Y. Foo, B. H. Hameed, *Chem. Eng. J,* **(2010)**, *156(1),* 2–10. **DOI:**10.1016/j.cej.2009.09.013
42. W. J. Weber Jr, J. C. Morris, *J. Saint. Eng Div,* **(1963)**, *89,* 31–42. **DOI:**10.1061/JSEDAI.0000430
43. Ali H. Jawad, Ahmed Saud Abdulhameed,M. A. K. M. Hanafiah, Zeid A. ALOthman, Mohammad Rizwan Khan, S. N. Surip, *Korean J of Chem Eng* (2021),*38*, 1499–1509. **DOI:**10.1007/s11814-021-0801-9
44. H. M. Guo, D. Stuben, Z. Berner, *Appl Geochem,* **(2007)**, *22(5),* 1039–1051. **DOI:**10.1016/j.apgeochem.2007.01.004

Povzetek

V tej študiji smo z uporabo metode odzivnih površin (RSM) z zasnovo Box-Behnkenovega načrtovanja optimizirali odstranjevanje As(V) iz vodnih raztopin s pripravljenim zamreženim ciklometilhitozanskim-epiklorhidrinskim/ Fe_3O_4 nanokompozitom. Optimizacijo pH vrednost raztopine, količine adsorbenta, kontaktnega časa in temperature smo izvedli s kvadratno polinomsko funkcijo z visokim korelacijskim koeficientom ($R^2 = 0.9406$). Ustreznost modela in izbranih členov smo preverili z analizo variance (ANOVA) in pokazali njihovo pomembnost z *F* – testom ($p < 0.05$). Izbrali smo sedem pomembnih členov s p-vrednostjo < 0.0001, na osnovi katerih smo določili optimum pri katerem je bila učinkovitost odstranjevanja As(V) 95.1 %, dosežena pri količini adsorbenta 0.7g, pH vrednosti 6.5, temperaturi 308K, koncentraciji arzena 10 mg/ml in kontaktnem času 60 min. Langmuirjev model, ki je z R^2 0.9988 in χ^2 0.1781 opisal eksperimentalne podatke bolje od Freundlichovega, kaže na maksimalno kapaciteto adsorpcije 28.99 mg/g. Proces kaže na enoplastno adsorpcijo in kinetiko psevdo-drugega reda. Termodinamski parametri kažejo, da je proces spontan in endotermen ter poteka fizikalna adsorpcija. Uspešna regeneracija adsorbenta kaže na njegov praktičen potencial pri odstranjevanju arzena iz onesnaženih voda.